Cerebral Cortex September 2009;19:2078–2091
doi:10.1093/cercor/bhn237
Advance Access publication March 10, 2009

Inactivation of the Somatosensory Cortex Prevents Paroxysmal Oscillations in Cortical and Related Thalamic Neurons in a Genetic Model of Absence Epilepsy

Pierre-Olivier Polack[1,2], Séverine Mahon[1,2], Mario Chavez[3] and Stéphane Charpier[1,2,4]

[1]INSERM UMR_S 667, Dynamique et Physiopathologie des Réseaux Neuronaux, F-75005 Paris, France, [2]Collège de France, UMR_S 667, F-75005 Paris, France, [3]Laboratoire de Neurosciences Cognitives & Imagerie Cérébrale, CNRS UPR 640 – LENA, 75651 Paris Cedex 13, France and [4]UPMC Univ Paris 06, UMR_S 667, F-75005 Paris, France

Absence seizures consist of bilateral spike-and-wave discharges (SWDs) occurring over widespread cortical and thalamic regions. In genetic models of absence epilepsy, recent in vivo investigations indicate that SWDs emerge first in the facial somatosensory cortex and then propagate via the corticothalamocortical loop. The specific involvement of this cortical region in ictogenic processes remained to be established and the participation of its related thalamocortical system in seizure initiation remained unclear. Here, using electrocorticographic (ECoG) and intracellular recordings in vivo from cortex and thalamus in the Genetic Absence Epilepsy Rat from Strasbourg (GAERS), we obtained novel evidence for the cortical focus theory of absence epilepsy. We report that blockade of action potential discharge and synaptic activities in facial somatosensory cortical neurons, by topical application of tetrodotoxin, prevents the occurrence of paroxysmal activities in local and distant cortical neurons and ECoGs, as well as in thalamocortical neurons in register with the somatosensory cortex. In contrast, pharmacological inhibition of a remote motor cortical region or of the related thalamic nuclei did not suppress ictal activities in the somatosensory cortex. This study demonstrates that SWDs in GAERS have a focal origin within the facial somatosensory cortex, which is sufficient and necessary to generate ictal activities.

Keywords: absence epilepsy, cortical inactivation, in vivo, somatosensory cortex, thalamus

Introduction

Absence epilepsy is an idiopathic nonconvulsive generalized epilepsy characterized by a sudden alteration of consciousness associated with bilateral 3- to 4-Hz spike-and-wave discharges (SWDs) in the electroencephalogram (Panayiotopoulos 1997). SWDs, in patients as well as in animal models of absence epilepsy, result from abnormal synchronized oscillations in corticothalamic networks (for review, see Danober et al. 1998; Timofeev and Steriade 2004). However, the specific contribution of cortical and thalamic neuronal elements in the initiation of spike-and-wave activity has long been a matter of debate (for review, see Timofeev and Steriade 2004; Meeren et al. 2005; van Luijtelaar and Sitnikova 2006).

Although earlier studies attributed the origin of SWDs to functional disturbances in intrathalamic neuronal networks (Buzsaki 1991; Bal et al. 1995; Avanzini et al. 2000), there is now growing evidence that the cerebral cortex exerts a prominent role in the generation and expression of spike-and-wave activity (Steriade and Contreras 1995; Seidenbecher et al. 1998; Steriade and Contreras 1998; D'Arcangelo et al. 2002; Meeren et al. 2002; Pinault 2003; Manning et al. 2004; Sitnikova and van Luijtelaar 2004; D'Arcangelo et al. 2006; Gurbanova et al. 2006; Polack et al. 2007). In particular, recent investigations in rodent models of absence epilepsy suggested that SWDs originate from a restricted region of the cerebral cortex (Meeren et al. 2002; Manning et al. 2004; Sitnikova and van Luijtelaar, 2004; Gurbanova et al. 2006; Polack et al. 2007). Nonlinear association analysis of cortical and thalamic electroencephalographic signals from the WAG/Rij rat, a genetic model of absence epilepsy (Coenen and van Luijtelaar 2003), revealed that SWDs were initiated in the peri-oral region of somatosensory cortex (Meeren et al. 2002). Electrical paroxysms recorded from other cortical sites, or the ventrobasal nuclei of the thalamus, consistently lagged those from this cortical region during the first 500 ms of the seizure (Meeren et al. 2002). Similarly, local field potentials recorded simultaneously from multiple cortical and thalamic sites in the Genetic Absence Epilepsy Rat from Strasbourg (GAERS; Danober et al. 1998) showed that paroxysmal electrical activities arise from the facial somatosensory cortex (Polack et al. 2007). Intracellular recordings from GAERS during absence seizures showed that paroxysmal discharges in layer 5–6 neurons of the facial somatosensory cortex systematically precede firing in distant cortical neurons (Polack et al. 2007). Moreover, these somatosensory cortex neurons fired at higher frequencies during interictal and ictal states and could generate between seizures short epochs of suprathreshold membrane oscillations, both consistent with an ictogenic role for this region of the cortex (Polack et al. 2007).

In both WAG/Rij rats and GAERS, SWDs were profoundly altered after systemic administration, or local application in the somatosensory cortex, of sodium channels blockers (lidocaine or phenytoin) (Sitnikova and van Luijtelaar 2004; Gurbanova et al. 2006). However, in these pharmacological studies, the effect of drugs on the neuronal activity within the somatosensory cortex was not assessed and the specific involvement of this cortical region in ictogenic activities was not demonstrated because the impact of an inactivation of other cortical areas was not tested.

Altogether, these data suggest that a cortical focus initiates absence seizures in GAERS and WAG/Rij rats. However, these findings do not demonstrate that somatosensory cortical neurons can generate paroxysmal discharges endogenously and are indispensible for the initiation and the generalization of SWDs, as expected for the "ictogenic neurons" of an epileptic focus. Moreover, the participation of the thalamus in seizure generation remains obscure because the activity of the thalamocortical neurons reciprocally connected with the cortical focus is still unknown.

Here, to directly assess the presumed specific ictogenic role of somatosensory cortical neurons, we examined in vivo in

GAERS the effects of a functional inactivation of somatosensory and motor cortical neurons on the occurrence of paroxysmal oscillations in cortical neurons, thalamocortical cells in register with the somatosensory cortex and surface electrocorticograms (ECoGs). We found that blocking neuronal discharges in somatosensory cortex by local application of tetrodotoxin (TTX) interrupted both local and distant surface SWDs. In contrast, inactivating motor cortex in the same way induced only a local suppression of SWDs, without affecting the ability of the somatosensory cortex to generate ictal activities. Moreover, we obtained evidence that thalamocortical neurons could not endogenously generate paroxysmal oscillations and were not required for the occurrence of SWDs in the somatosensory cortex. First, the functional inactivation of the somatosensory cortex prevented paroxysmal discharges in the related thalamocortical neurons. Second, cortical SWDs were not systematically correlated with neuronal oscillations in the thalamus. Finally, suppression of thalamic epileptic oscillations following intrathalamic injection of TTX did not prevent cortical spike-and-wave activity.

This demonstration of the specific capacity of facial somatosensory cortical neurons to produce ictal discharges, and their key role in the generation of distant cortical and thalamic paroxysmal activity, provide direct evidence for the "cortical focus" theory of "generalized" absence epilepsy.

Material and Methods

Animal Preparation

All experiments were performed in accordance with local Ethical Committee and European Union guidelines (directive 86/609/EEC), and every precaution was taken to minimize stress and the number of animals used in each series of experiments.

Experiments were performed in vivo on 28 adult (>15 weeks) male and female GAERS. Animals were initially anaesthetized with sodium pentobarbital (40 mg/kg, i.p.; Sanofi, Libourne, France) and ketamine (100 mg/kg, i.m.; Imalgène, Merial, France). A cannula was inserted into the trachea, and the animal was placed in a stereotaxic frame. Wounds and pressure points were repeatedly (every 2 h) infiltrated with lidocaine (2%). Once the surgical procedures had been completed (see below), analgesics were applied and rats were maintained in a narcotized, sedated state by injections of fentanyl (3 μg/kg, i.p.; Janssen-Cilag, Issy-les-Moulinaux, France) repeated every 20–30 min (Simons and Carvell 1989; Pinault et al. 1998; Charpier et al. 1999; Slaght et al. 2002; Bruno et al. 2003; Slaght et al. 2004). To obtain long-lasting stable intracellular recordings, rats were immobilized with gallamine triethiodide (40 mg i.m. every 2 h; Specia, Paris, France) and artificially ventilated. The degree of anesthesia was assessed by monitoring the ECoG and heart rate. Additional doses of fentanyl were administered if there were any signs of arousal such as an increase in the frequency and reduction in the amplitude of ECoG waves or an increase in the heart rate. Body temperature was maintained (36.5–37.5 °C) with a homeothermic blanket. At the end of the experiments, animals received an overdose of sodium pentobarbital (200 mg/kg, i.p.).

Electrophysiological Recordings

ECoG recordings were made with low impedance (~60 kΩ) silver electrodes placed on the dura above one or both facial somatosensory cortices (8.5–9.0 mm anterior to the interaural line; 7.0 mm lateral to the midline) and orofacial motor cortex (12 mm anterior to the interaural line; 3.5–4 mm lateral to the midline) (Paxinos and Watson 1986). Reference electrodes were placed in a contralateral head muscle.

Intracellular recordings were obtained with glass micropipettes filled with 2M potassium acetate (50–70 MΩ). Cortical cells of the facial somatosensory cortex were recorded at sites anterior to the local ECoG electrode at the following coordinates: 8.5–9.0 mm anterior to the interaural line, 5.0–5.5 mm lateral to the midline, and 1.4–3.8 mm under the cortical surface. Cortical cells located in the orofacial motor cortex were recorded close to the local ECoG electrode at the following coordinates: 12 mm anterior to the interaural line, 3.6–3.8 mm lateral to the midline, and 0.9–2 mm under the cortical surface. The depths of cortical intracellular records, in both somatosensory and motor cortices, indicate that recorded cells were located in the layers 5–6 (deep layers). Intracellular recordings of thalamic relay neurons were made from the ventro-posterior medial (VPM) and posterior medial (POm) nuclei in register with the facial somatosensory cortex (see Results). The corresponding stereotaxic coordinates were: 5.2–5.4 mm anterior to the interaural line, 2.5–2.8 mm lateral to the midline, and 5.2–6.0 mm (VPM) or 4.5–5.2 mm (POm) ventral to the brain surface.

In all experiments, intracellular recordings were coupled with ECoG recordings from ipsilateral somatosensory and motor cortices. In some experiments (see Fig. 3), intracellular activity of somatosensory cortical neurons was monitored simultaneously with ECoG recordings from both ipsi- and contralateral somatosensory cortices.

TTX Experiments

The sodium channel blocker TTX (1mM TTX, tetrodotoxin citrate in 0.9% saline, Tocris, UK) was applied by topical superfusion (50–100 μL) to the cortical surface, close to the intracellular pipette, in order to completely suppress the local generation of action potentials. The disappearance of synaptic and firing activities in deep-layer cortical neurons was used to assess the progress of this inactivation during TTX superfusion. In separate experiments, TTX was either applied above facial somatosensory cortex or orofacial motor cortex and its effect was determined on the occurrence of SWDs in ECoG recordings. Assuming an isotropic diffusion of the drug (Myers 1966; Papadopoulos et al. 2005), the diffusion velocity was calculated in each experiment from the depth of the intracellular recording and the time until action potential and synaptic activity was completely blocked in the recorded cortical neurons. These estimates of the time needed for TTX diffusion to recorded sites provided assurance that actions at greater distances did not result from an intracerebral spread of the drug.

Intrathalamic injections of TTX (30 μL, 100μM) were made via a steel cannula (tip diameter, 250 μm) fitted to a 50-μL Hamilton syringe inserted at the boundary between the POm and VPM nuclei, with the following stereotaxic coordinates: 5.4 mm anterior to the interaural line, 2.5 mm lateral to the midline, and 5.5 mm ventral to the brain surface. The corresponding thalamic local field potential was monitored by a thin (125 μm of diameter) silver electrode cemented to the injection cannula and the ipsilateral somatosensory ECoG was simultaneously recorded (see above).

Anatomical Procedures

Microiontophoretic injections of wheatgerm agglutinin–horseradish peroxidase complex (WGA-HRP, 2.5% in 0.9% saline; Sigma) were made in the facial somatosensory cortex (8.5 mm anterior to the interaural line, 5.5 mm lateral to the midline, 2.5 mm ventral to the brain surface) using glass micropipettes of internal tip diameter 15 μm and positive current pulses of 5 μA for 10 min. Following a survival period of 48 h, animals were deeply anaesthetized with pentobarbital (100 mg/kg, i.p.) and intracardially perfused with 100 mL of 0.9% saline followed by 500 mL of 3.5% glutaraldehyde in 0.1M phosphate buffer (PB) (pH 7.4) and 200 mL of a 10% sucrose solution in 0.1M PB (pH 7.4). Brains were removed and stored overnight in this buffer before cutting frontal sections with a freezing microtome. Sections were processed for histochemistry using the tetramethyl benzidine method of Mesulam (1978), mounted on chrome-alum-coated slides and counterstained with safranin. Injection sites and retrogradely labeled neurons were observed under bright-field illumination.

Intracellularly recorded neurons were labeled using 1% neurobiotin (Vector Laboratories, Burlingame, CA) added to the intracellular solution. 1–2 h after the injection, the animal received a lethal dose of pentobarbital and was perfused with 500 mL of a physiological solution followed by 500 mL of 0.3% glutaraldehyde and 4% paraformaldehyde in 0.1M PB (pH 7.4). Brains were postfixed for 2 h in the same fixative solution without glutaraldehyde and then immersed in

30% sucrose PB at 4 °C until sectioning. Frozen sections of fixed brains were cut at 50–70 μm in the frontal plane and serially collected in PB. Neurobiotin was revealed by incubating sections in the avidin–biotin peroxidase complex (1:100; Vector Laboratories) in PB containing 0.3%Triton X-100 for at least 12 h at 4 °C. Sections were then immersed in a solution containing 0.005% 3,3'-diaminobenzidine tetrahydrochloride (Sigma, St Louis, MO), 0.4% nickel-ammonium sulfate, and 0.0006% H_2O_2. After several rinses in PB, sections were mounted on gelatin-coated slides, counterstained with safranin, and dehydrated through alcohol to xylene for light microscopic examination. The location of labeled neurons within the VPM and POm thalamic nuclei was confirmed using the atlas of Paxinos and Watson (Paxinos and Watson 1986).

Data Acquisition and Analysis

Intracellular recordings were obtained under current-clamp conditions using the active bridge mode of an Axoclamp-2B amplifier (Molecular Devices, Union City, CA). Data were stored on-line on a DRA 800 digital tape recorder (Biologic, Claix, France) and digitized for analysis at a sampling rate of 10 kHz for the intracellular signal and 1 kHz for the ECoG. Measurements of apparent membrane input resistance and time constant were based on the linear electrical cable theory applied to an idealized isopotential neuron (Rall 1969). Apparent membrane input resistance was measured from the linear portion of the voltage–current (V–I) relationships or from the mean ($n \geq 10$) membrane potential change at the end of hyperpolarizing current pulses of low intensity (–0.4 nA, 200 ms duration, applied every 1.25 s). The membrane time constant was determined from an exponential fit to the hyperpolarization. Average membrane potential of cortical and thalamic neurons was determined during interictal periods, from continuous recordings of at least 5 s. Membrane potential values were corrected by subtracting the extracellular tip potential measured immediately after the loss of intracellular recordings.

The beginning (or the end) of a SWD was taken as the first (or the last) spike-wave complex, with amplitude for the spike of at least 2 times the peak-to-peak amplitude of baseline ECoG fluctuations (Polack et al. 2007). Spectral analysis of the ECoG was performed with fast Fourier transforms applied using Spike 2 software (Cambridge Electronic Design, Cambridge, UK). The amplitude of action potentials was calculated as the potential difference between their voltage threshold, measured as the membrane potential at which the dV/dt exceeded 10 V x s^{-1} (Fricker et al. 1999; Mahon et al. 2003), and the peak of the spike. Numerical values are given as means ± SEM. Statistical significance was assessed with appropriate statistical tests, Student's paired or unpaired *t* test, one-way ANOVA and Mann–Whitney rank sum test. Statistical analysis and curve fitting were performed with Origin 6.0 (OriginLab Corp., Northampton, MA) and SigmaStat 3.0 (SPSS Inc., Chicago, IL).

Results

Deep-Layer Somatosensory Cortical Neurons Lead Spike-and-Wave Activity

We recorded in vivo in GAERS the intracellular activity of neurons located in deep layers of the facial part of the somatosensory cortex (Fig. 1*A*) or of the orofacial motor cortex (Fig. 1*B*), simultaneously with the ECoG activities of the related cortical regions. Spontaneous episodes of SWDs had a mean duration of 11.1 ± 0.6 s (n = 1084 SWDs from 23 GAERS) with interictal periods of 15.3 ± 1.1 s (n = 1055 SWDs from 23 GAERS). The mean frequencies of oscillations during surface paroxysms recorded from the somatosensory (8.0 ± 1.1 Hz, n = 1084 SWDs from 23 GAERS) and motor (7.8 ± 1.0 Hz, n = 1084 SWDs from 23 GAERS) areas were not significantly different ($P > 0.5$; unpaired *t*-test). These temporal properties of SWDs, as well as the shape of individual spike-wave complexes, were similar to those previously reported in similar experimental conditions (Pinault et al. 1998; Pinault 2003; Slaght et al. 2004; Paz et al. 2007; Polack et al. 2007) as well as in freely moving GAERS (Marescaux et al. 1992; Deransart et al. 2003; Polack et al. 2007).

During interictal periods, somatosensory cortical neurons fired at a high frequency (31.6 ± 5.9 Hz, n = 10 cells) associated with a sustained membrane depolarization (–56.2 ± 0.7 mV, n = 10 cells) (Fig. 1*A*). SWDs were associated with suprathreshold rhythmic depolarizations of somatosensory cortical neurons (Fig. 1*A*) superimposed on a tonic membrane hyperpolarization (8.5 ± 0.9 mV, n = 10 cells) lasting for the entire SWD (Fig. 1*A*). Virtually all ECoG spikes were associated with 1–8 action potentials (firing probability = 0.99 ± 0.01, n = 161 SWDs from 10 cells) corresponding to a mean ictal firing rate of 25.9 ± 5.1 Hz (n = 10 cells) (Fig. 1*A*, *C*, and *D*).

Between SWDs, cortical motor neurons (Fig. 1*B*) exhibited, a less depolarized membrane potential (–60.3 ± 0.9 mV, n = 7 cells; $P < 0.01$; unpaired *t*-test) and a lower firing rate (6.9 ± 1.4 Hz, n = 7 cells; $P < 0.01$; unpaired *t*-test) than somatosensory cortical neurons. They were also less likely to fire in association with ECoG spikes during SWDs (probability 0.34 ± 0.07, n = 7 cells; $P < 0.01$; unpaired *t*-test) (Fig. 1*B*, *C*, and *D*).

Temporal relations between the firing of deep-layer somatosensory and motor cortical neurons during SWDs were determined by measuring the timing (Δt) of individual action potentials relative to the peak negativity of the corresponding spike component in the somatosensory ECoG (Fig. 1*C*). Throughout seizures, somatosensory cortical neurons consistently fired before motor neurons. Action potential latencies in somatosensory and motor cortical neurons were unimodally distributed, with a mean delay of –17.9 ms ± 0.1 ms (n = 20 301 action potentials from 161 SWDs, n = 10 cells) and –5.7 ± 0.6 ms (n = 1885 action potentials from 55 SWDs, n = 7 cells), respectively (Fig. 1*D*).

These results confirm that deep-layer neurons of the somatosensory cortex are hyperactive compared with other cortical cells (Polack et al. 2007) and support their leading role during SWDs.

Inactivation of Somatosensory Cortical Neurons Prevents Generalized Spike-and-Wave Activity

The role of deep-layer somatosensory cortical neurons in the initiation and generalization of ictal activities was first examined by studying the effects of the inactivation of these cells on the occurrence of SWDs in local and distant cortical regions.

Blockade of activity in somatosensory cortical neurons was obtained 20 min after topical application of TTX to the cortical surface. The efficacy of this treatment was confirmed by recording the intracellular activity of underlying deep-layer cortical neurons (Fig. 2*A*). Cessation of local ECoG spike-and-wave activity was correlated with the blockade of spontaneous (Fig. 2*A*) and current-evoked (Fig. 2*B*) action potentials in individual cortical neurons. As expected from the interruption of propagated activity in the related synaptic networks, there was a dramatic decrease in the number and amplitude of membrane potential fluctuations in recorded cells (Fig. 2*Ab*, *Bb*, and *C*). We quantified the alteration in membrane potential fluctuations, partly due to spontaneous synaptic inputs, by comparing the standard deviation of interictal membrane potential values in control and after TTX application. Across cells (n = 5), this parameter was reduced from 6.5 ± 0.9 mV to

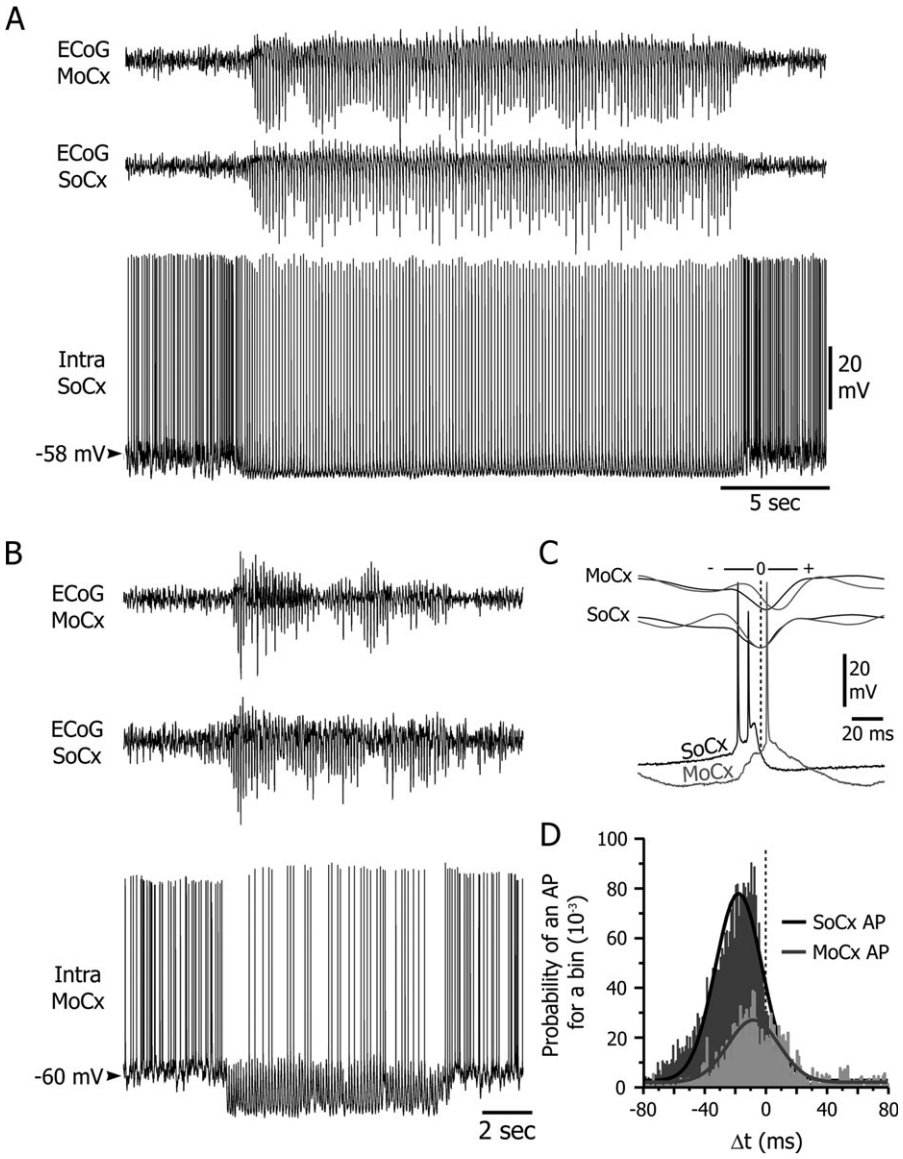

Figure 1. Deep-layer neurons of the somatosensory cortex lead cortical spike-and-wave activity. (*A*) and (*B*) Intracellular activity (lower traces) of a layer V somatosensory (*A*, Intra SoCx) and motor (*B*, Intra MoCx) cortical neuron simultaneously recorded with the corresponding somatosensory (ECoG SoCx, middle trace) and motor (ECoG MoCx, top trace) ECoGs during a spontaneous SWD. Note the elevated ictal and interictal firing rate characteristic of the deep-layer somatosensory cortical neurons in GAERS (see also Polack et al. 2007). (*C* and *D*) Temporal relationship between action potential discharge in somatosensory and motor cortical neurons during SWDs. (*C*) Superimposition of suprathreshold depolarizations (bottom) recorded from somatosensory (black trace) and motor (gray trace) cortical neurons and the corresponding somatosensory (middle traces) and motor (top traces) spike-wave complexes. The peaks of the somatosensory ECoG spikes were used to align the records. (*D*) Pooled distribution of the timing (Δt) of all action potentials (AP; bin size, 1 ms) recorded in somatosensory (dark gray bars, $n = 20\,301$ action potentials from 10 cells) and in motor (light gray bars, $n = 1885$ action potentials from 7 cells) cortical neurons relative to the peak of the somatosensory ECoG spike, which was taken as the zero-time reference (*C*). The distributions were best fitted by single Gaussian curves ($r^2 = 0.941$ for both fits). The mean latency of the first action potential was -26.5 ± 0.2 ms for SoCx neurons ($n = 10$ cells) and -6.9 ± 0.6 ms ($n = 7$ cells) for MoCx neurons. Here and in the following figures, the value of membrane potential is indicated at the left of the intracellular record. The voltage calibration in (*A*) applies to (*B*).

0.5 ± 0.1 mV ($P < 0.05$; Mann–Whitney rank sum test) (Fig. 2*C*). The effective blockade of network activities within the somatosensory cortex was also demonstrated by a considerable reduction in the power of high frequencies (>10 Hz) in the corresponding ECoG signal (Fig. 2*D*).

TTX-induced changes in network activity were associated with modifications in the membrane electrical properties of affected cells. As previously reported (Pare et al. 1998; Destexhe and Pare 1999), a pronounced drop in membrane potential (Control, –56.2 ± 0.7 mV, $n = 10$ cells; after TTX, –67.9 ± 1.1 mV, $n = 5$ cells; $P < 0.01$; unpaired *t*-test; Fig. 2*A–C*) and an increase in the apparent input resistance (Control, 17.5 ± 2.2 MΩ, $n = 10$ cells; after TTX, 25.2 ± 1.6 MΩ, $n = 5$ cells; $P < 0.05$; unpaired *t*-test) were observed after TTX application (Fig. 2*B*).

We next investigated the impact of the inactivation of facial somatosensory cortical neurons on the incidence of SWDs in distant cortices ($n = 5$ experiments). As shown in Figures 1*Aa*, 2*Aa*, and 3*Aa*, the transition from interictal to ictal states was correlated with the appearance of rhythmic clusters of action potentials in deep-layer somatosensory cortical neurons (Fig. 3*Aa*) and generalized spike-wave complexes at ~7.5 Hz

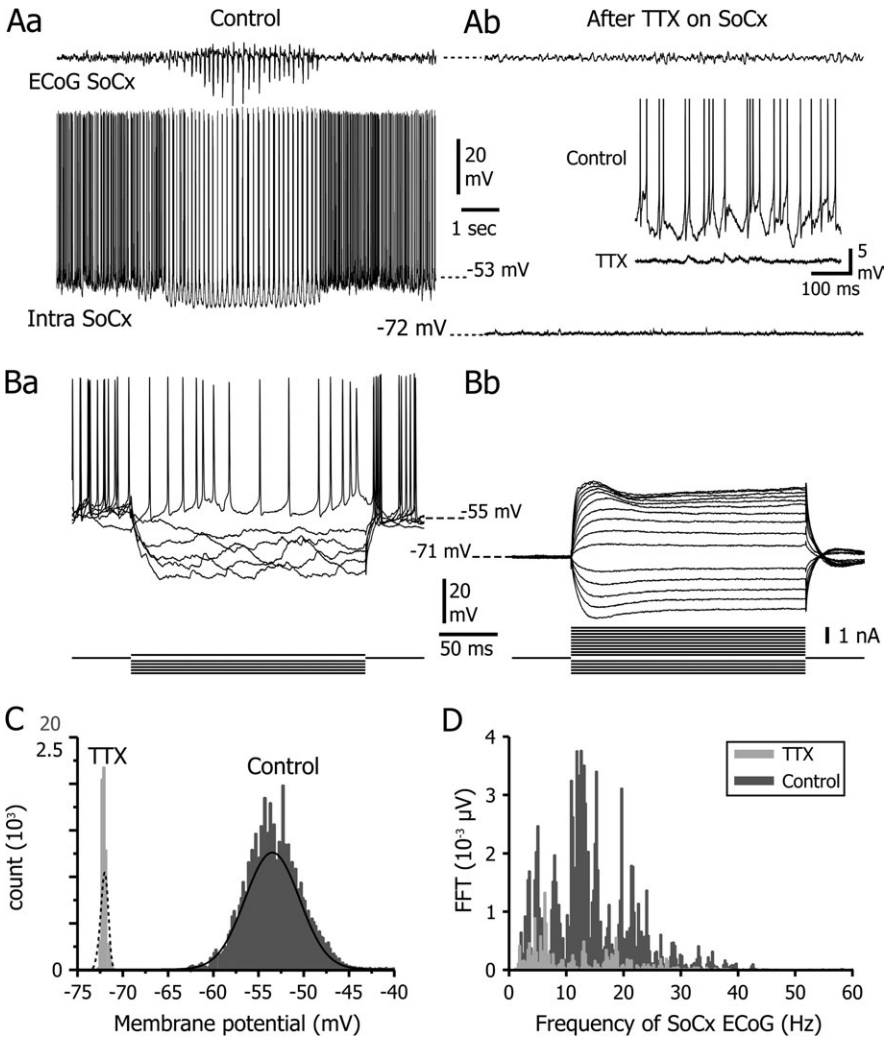

Figure 2. ECoG and intracellular activities from the somatosensory cortex before and after local application of TTX. (*A*) Intracellular activity of a deep-layer neuron from the somatosensory cortex (bottom trace) simultaneously recorded with the corresponding ECoG (ECoG SoCx, top trace), before (Control, *Aa*) and after (*Ab*) surface application of TTX. *Ab*, the disappearance of local SWDs was concomitant in the recorded cell with the occlusion of spontaneous action potentials and ongoing synaptic activity. Inset, expansion of short periods of intracellular activities in control and after TTX application. Action potentials in the control record have been truncated for clarity. (*B*) Voltage responses (top traces) of the neuron shown in *A* to hyperpolarizing and depolarizing current pulses (bottom traces), before (*Ba*) and during (*Bb*) TTX treatment. A pronounced outward rectification in the depolarizing direction was revealed after blockade of sodium channels. (*C*) Distributions of the membrane potential values (bin = 0.2 mV; continuous record of 5 s) during interictal periods in control conditions (control) and after application of TTX. Both distributions were best fitted by unimodal Gauss–Laplace fits (Control, continuous line, center = −53.5 ± 5.9 mV, r^2 = 0.736; TTX, dashed line, center = −72.1 ± 0.4 mV, r^2 = 0.974). (*D*) Fast Fourier Transform (FFT) performed on the somatosensory ECoG during interictal periods, in control (control, black) and after drug application (TTX, gray). All results depicted in this figure are from the same neuron.

(Fig. 3*Aa* and *Ba*). After TTX application, the suppression of cellular activity in the somatosensory cortex resulted in the concomitant disappearance of SWDs in ipsilateral somatosensory and motor cortices (Fig. 3*Ab*).

In 4 experiments, we examined the effects of unilateral application of TTX to somatosensory cortex on ECoG activity in the contralateral homotypic region. Contralateral SWDs (Fig. 3*Aa*, top trace) were replaced by periods of residual "ictal-like" oscillations (Fig. 3*Ab*, top trace), of shorter duration (9.1 ± 4.3 s, n = 4; P < 0.05 for each experiment; Mann–Whitney rank sum test) and longer interictal periods (100.6 ± 46.3 s, n = 4; P < 0.05 for each experiment; Mann–Whitney rank sum test), than full-blown SWDs (control duration, 24.5 ± 7.3 s; control inter-SWD interval = 23.1 ± 11.2 s, n = 4). Moreover, in this set of experiments, the internal frequency of residual oscillations (7.9 ± 0.3 Hz, n = 4) was slightly but significantly (P < 0.05 for each experiment; Mann–Whitney rank sum test) increased from the control frequency during SWDs (7.3 ± 0.2 Hz, n = 4) (Fig. 3*B*, top panels). This remaining "ictal-like" activity was completely abolished after local application of TTX to the contralateral somatosensory cortex (result not shown).

Inactivation of Motor Cortex Neurons Does Not Alter the Occurrence of SWDs in the Somatosensory Cortex

The fact that pharmacological inactivation of somatosensory cortical neurons prevents generalized SWDs does not demonstrate that this region is specifically involved in seizure initiation. It could simply indicate that the functional integrity of the cortex is required for the initiation and expression of ictal activities. Thus, we directly assessed the putative ictogenic role for somatosensory cortex by testing, for the first time (see

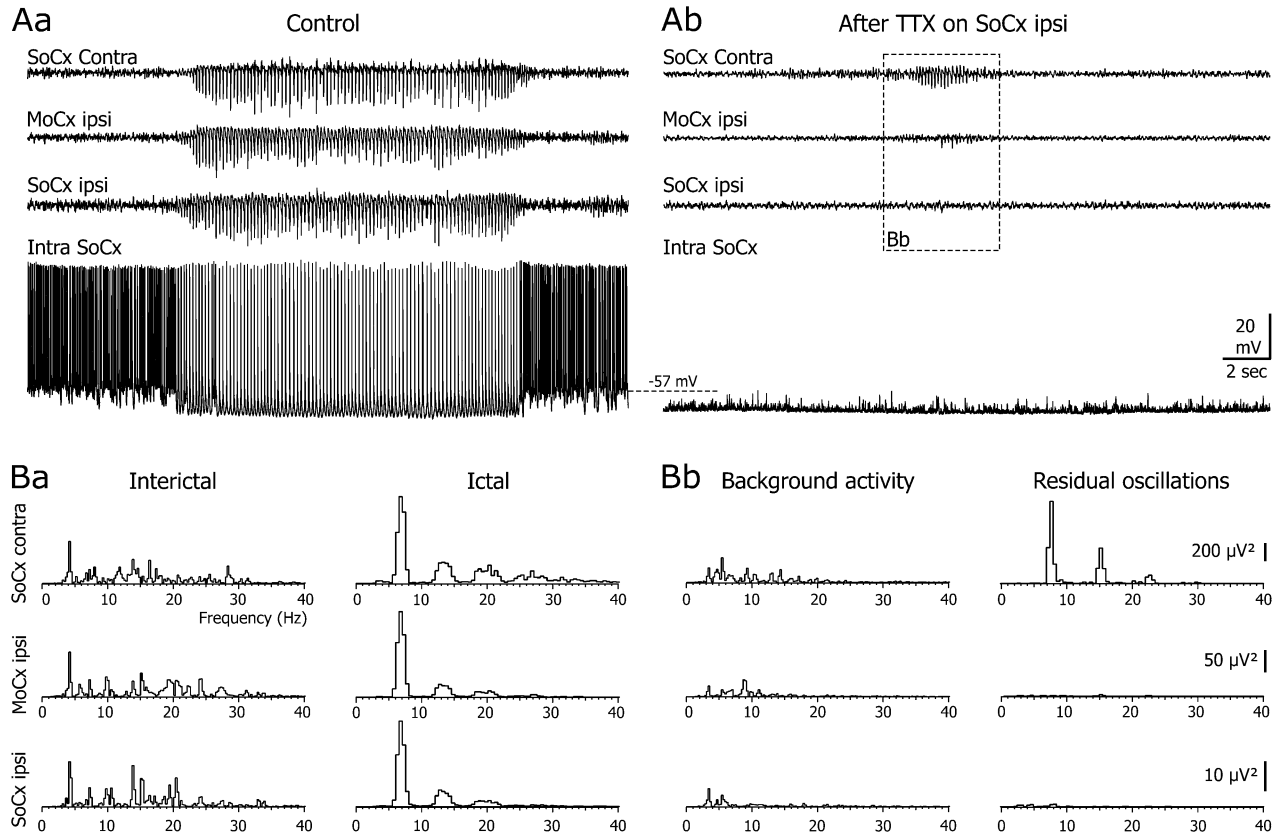

Figure 3. Impact of TTX application on the somatosensory cortex upon spike-and-wave activity. (*A*) Intracellular activity of a deep-layer neuron of the somatosensory cortex (bottom trace) simultaneously recorded with the ECoG waves from ipsilateral somatosensory cortex (SoCx ipsi), motor cortex (MoCx ipsi) and contralateral somatosensory cortex (SoCx contra), before (*Aa*) and after (*Ab*) application of TTX on the ipsilateral somatosensory cortex. Note that TTX affected spike-and-wave activity in all ECoG records. (*B*) Power spectra of the ECoG signals shown in *A*, before (*Ba*) and after TTX application (*Bb*). In control conditions (*Ba*), spectral analyses were performed in between (Interictal) and during (Ictal) SWDs. After TTX application (*Bb*), the spectral profile of ECoG records was determined in between (Background activity) and during (Residual oscillations) periods of residual oscillations, which were prominent only in the contralateral somatosensory cortex (dashed box in *Ab*). All results illustrated in this figure are from the same quadruple recording.

Sitnikova and van Luijtelaar 2004; Gurbanova et al. 2006), its capacity to generate paroxysmal discharges during partial synaptic deafferentation. In 5 experiments, we examined how the inactivation of motor cortex neurons affected the incidence of local and somatosensory cortical SWDs, which were recorded at a distance of 5.2 mm from the site of drug application. Intracellular activity of neurons from deep layers of motor cortex was recorded simultaneously with the motor and ipsilateral somatosensory ECoGs, before (Fig. 4*Aa*) and during TTX application to the motor cortex (Fig. 4*Ab*). As observed in somatosensory cortex, after 10 min of diffusion TTX suppressed spontaneous action potential discharge and synaptic activity in motor cortex neurons, producing a significant membrane hyperpolarization (Control, –60.3 ± 0.9 mV, n = 7 cells; after TTX, –68.5 ± 2.0 mV, n = 6 cells; $P < 0.01$; unpaired t-test) (Fig. 4*Ab*). As illustrated in Figure 4*B*, TTX abolished the generation of action potentials by current injections and caused a small increase in the apparent input resistance (Control, 21.4 ± 3.7 MΩ, n = 7 cells; after TTX, 24.8 ± 3.8 MΩ, n = 6 cells; P = 0.54; unpaired t-test).

The interruption of activity in motor cortical networks resulted in the cessation of SWDs in the local surface ECoG, but paroxysmal discharges in the ipsilateral somatosensory cortex remained unchanged (Fig. 4*Ab*). Somatosensory SWDs after TTX-induced inhibition of the motor cortex had a duration (23.7 ± 14.0 s, n = 117 SWDs from 5 experiments), an internal frequency (8.1 ± 0.4 Hz, n = 117 SWDs from 5 experiments) and a mean interictal period (16.6 ± 2.6 s, n = 114 SWDs from 5 experiments) similar ($P > 0.05$ for each parameter; unpaired t-test) to those calculated during the corresponding control conditions.

We can exclude that the disappearance of SWDs in motor cortex after TTX application on the somatosensory area was due to a spread of the drug. First, the velocities of TTX diffusion when applied on the somatosensory (1.8 µm/s) and motor (2.1 µm/s) cortices were similar ($P > 0.5$; unpaired t-test). Second, the blockade of SWDs in the motor cortex was concomitant with the inactivation of the somatosensory cortex whereas epileptic discharges were recorded in the somatosensory cortex after inactivation of the motor region.

Morphofunctional Properties of Thalamocortical Neurons Projecting to the Somatosensory Cortex

Thalamocortical neurons could contribute to the appearance of epileptic discharges in the somatosensory cortex. We assessed possible participation of thalamocortical inputs in the initiation of seizures, by comparing the intracellular activity of thalamic neurons projecting to the facial somatosensory cortex in

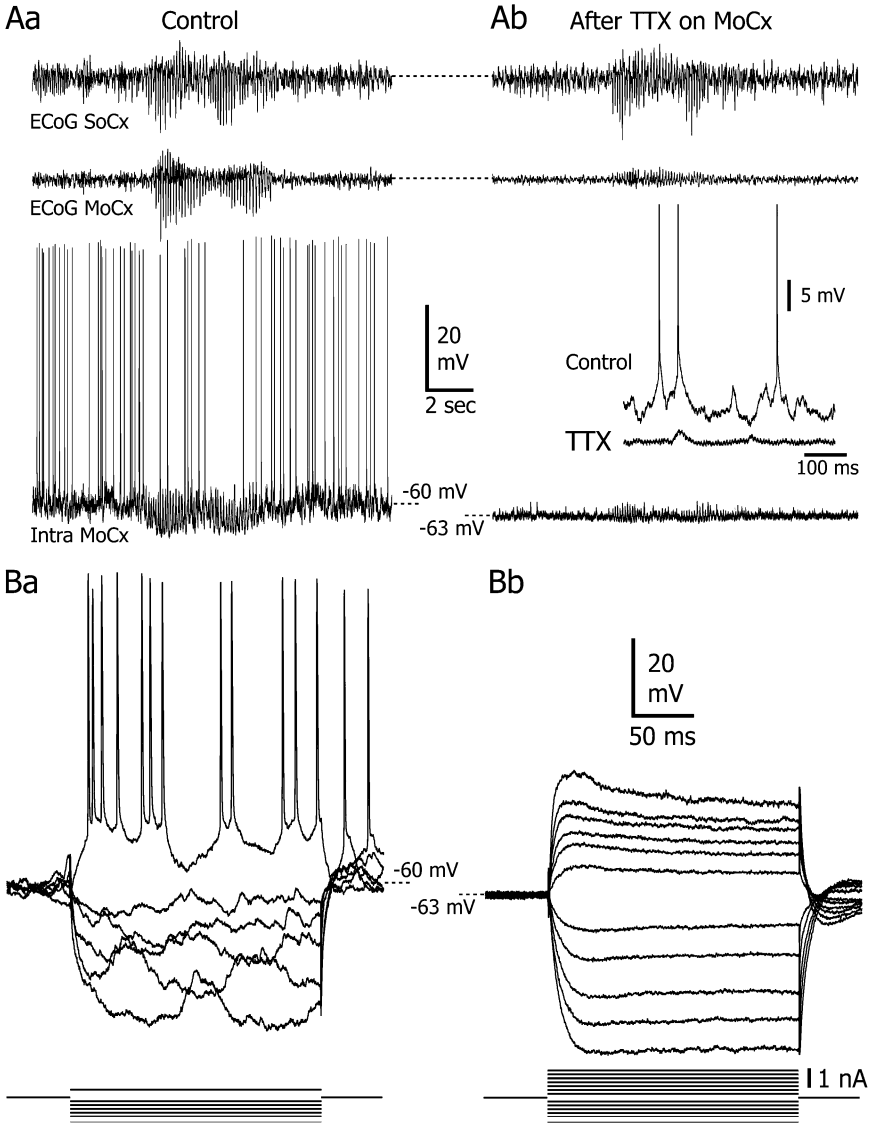

Figure 4. Local application of TTX on the motor cortex does not affect the occurrence of SWDs in the somatosensory cortex. (*A*) Intracellular activity of deep-layer motor cortex neuron simultaneously recorded with the corresponding ECoGs from the motor (MoCx) and ipsilateral somatosensory (SoCx) cortices, before (*Aa*) and after (*Ab*) topic application of TTX on the motor cortex. SWDs persisted in the somatosensory cortex whereas they were abolished in the motor region. Inset, expanded periods of the intracellular activity, in control and after TTX treatment. Action potentials in the control record are truncated for clarity. (*B*) Voltage responses (top traces) of the same neuron to hyperpolarizing and depolarizing current pulses (bottom traces), before (*Ba*) and after (*Bb*) application of TTX.

control conditions and during pharmacological inhibition of the ipsilateral somatosensory cortex.

Injections of WGA–HRP in the facial somatosensory cortex were performed to determine the location of cells providing their thalamocortical inputs (Fig. 5*Aa*). Consistent with previous anatomical studies (Emmers 1988), the somata of retrogradely labeled thalamocortical neurons were situated in the medioventral part of the POm thalamic nucleus and in the VPM thalamic nucleus (Fig. 5*Ab* and *Ac*). VPM and POm thalamic cells intracellularly labeled with neurobiotin exhibited typical morphological features of thalamocortical relay neurons (Sawyer et al. 1989; Steriade et al. 1997), including a fusiform perikaryon with at least 3–7 visible stout proximal dendrites, which branched to form more slender distal dendrites (Fig. 5*Ba* and *Ca*, bottom panels).

As classically described for relay thalamic cells (Steriade et al. 1997; Sherman 2001; Destexhe and Sejnowski 2003), VPM and POm thalamic neurons fired tonically in response to depolarizing current pulses applied from the resting potential (Fig. 5*Bb* and *Cb*). VPM thalamic neurons had a slightly higher apparent input resistance (VPM, 45.0 ± 5.7 MΩ, $n = 4$ cells; POm, 34.7 ± 2.6 MΩ, $n = 7$ cells; $P = 0.09$; unpaired *t*-test) and a shorter membrane time constant (VPM, 8.4 ± 0.9 ms, $n = 4$ cells; POm 17.0 ± 2.3 ms, $n = 7$ cells; $P < 0.05$; unpaired *t*-test), than POm neurons. Both cell types exhibited, in response to negative current pulses of high intensity, a slow depolarizing sag (Fig. 5*Bb* and *Cb*) indicative of the presence of the hyperpolarization-activated inward cationic current I_h (McCormick and Pape 1990). Large-amplitude current-induced hyperpolarizations were systematically followed by a rebound depolarization (Fig. 5*Bb* and *Cb*), likely resulting from I_h (McCormick and Pape 1990; Destexhe and Sejnowski 2003) and/or from the low-threshold activated calcium current (I_T) (Jahnsen and Llinás 1984a, 1984b; Steriade et al. 1997; Destexhe and Sejnowski 2003).

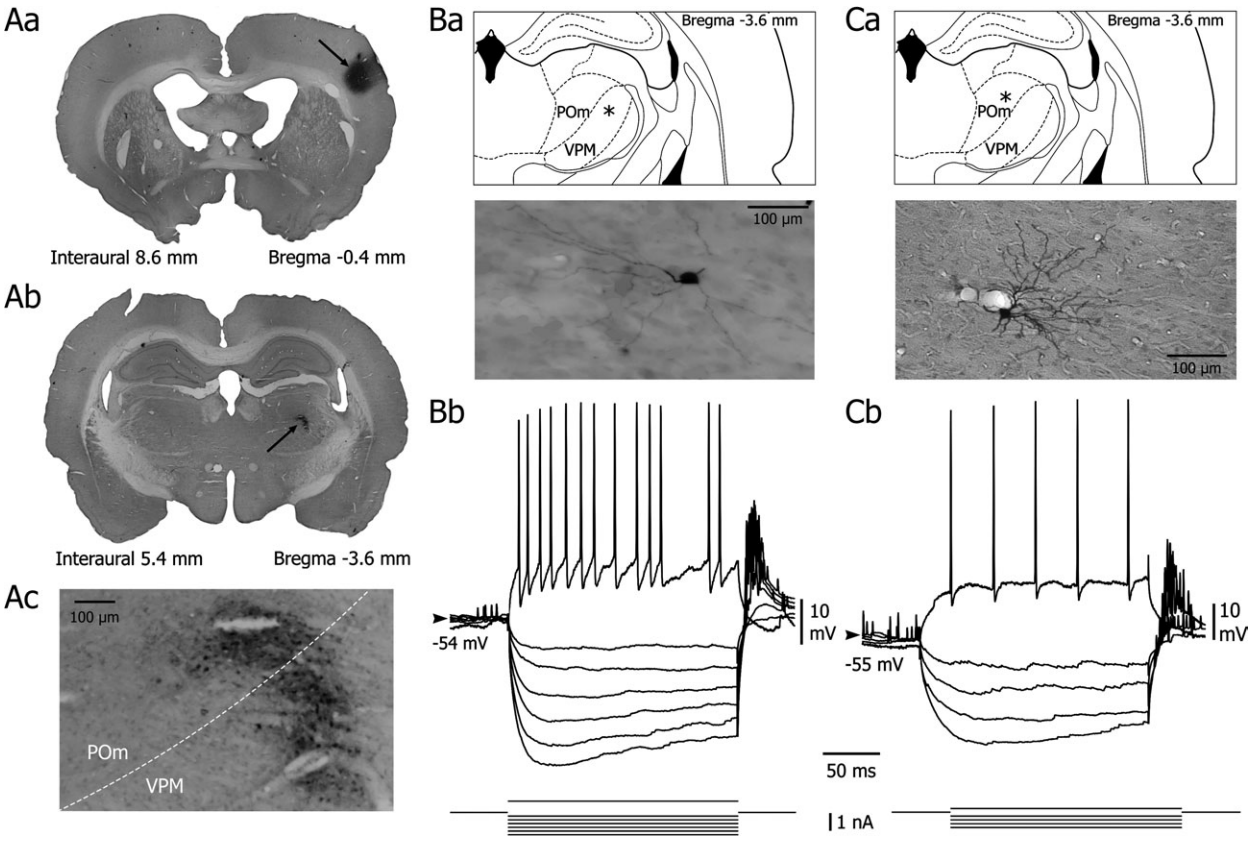

Figure 5. Morphofunctional properties of thalamic relay neurons projecting to the facial region of the somatosensory cortex. (*A*) Location of retrogradely labeled neurons in the thalamus after WGA–HRP injection in the facial region of the somatosensory cortex. (*Aa*) Microphotograph of the WGA–HRP injection site (arrow) in the somatosensory cortex at the indicated anteriority. (*Ab*) Microphotograph of a coronal section (anteriority: 5.4 mm with respect to the interaural line) showing the spatial distribution of the retrogradely labeled thalamic neurons (arrow). As shown by the expanded view, thalamic neurons were located in the VPM and POm thalamic nuclei (*Ac*). (*Ba* and *Ca*) Schematic localization (top) and microphotographs (bottom) of a VPM (*Ba*) and a POm (*Ca*) thalamic neurons intracellularly filled with neurobiotin. Asterisks in top panels indicate the position of the corresponding cell bodies. The fusiform perikaryons and the numerous varicose dendrites are characteristic of thalamocortical neurons (bottom panels). (*Bb* and *Cb*) Voltage responses (top traces) to hyperpolarizing and depolarizing current pulses (bottom traces) of the thalamic neurons shown in (*Ba*) and (*Ca*), respectively. The responses induced by hyperpolarizing current pulses are an average of 10 successive trials.

Activity of Thalamocortical Neurons during SWDs

VPM and POm thalamic neurons had similar mean interictal membrane potentials (VPM, –57.7 ± 1.4 mV, n = 4 cells; POm, –58.0 ± 1.4 mV, n = 7 cells; P > 0.05; unpaired t-test) and discharged action potentials irregularly at low frequencies between seizures (VPM, 2.0 ± 1.0 Hz, n = 4 cells; POm, 0.5 ± 0.2 Hz, n = 7 cells; P > 0.05; unpaired t-test) (Fig. 6*A*,*B*).

Spontaneous transitions between interictal and ictal periods were accompanied in VPM thalamic neurons by membrane potential oscillations, temporally correlated with spike-wave complexes in the ECoG and superimposed on a large tonic hyperpolarization (10.6 ± 0.3 mV, n = 32 SWDs from 4 cells; Fig. 6*A*). In all recorded VPM neurons, single action potentials were triggered on SWD-associated rhythmic membrane depolarizations (Fig. 6*C*, VPM), with a low probability of firing (0.12 ± 0.09, n = 517 action potentials from 32 SWDs) in association with each ECoG spike. In contrast, POm neurons exhibited a large-amplitude (15.5 ± 0.8 mV, n = 39 SWDs from 7 cells) asymmetric hyperpolarizing envelope during SWDs (Fig. 6*B*). It was associated with robust membrane oscillations that could trigger bursts of action potentials (Fig. 6*C*, *POm*). During SWDs, all POm neurons could fire action potentials and their mean firing rate was 1.3 ± 0.4 Hz (n = 7 cells), corresponding to a firing probability in association with each ECoG spike of 0.16 ± 0.04 (n = 7 cells).

The temporal relationship between the firing of somatosensory cortical neurons and related thalamic cells during SWDs was first determined by measuring action potential timing relative to the peak negativity of the somatosensory ECoG spike (Fig. 6*C*). Action potentials were generated in both groups of thalamic cells before the peak of the ECoG spike (–9.2 ± 0.7 ms, n = 71 SWDs from 11 VPM-POm cells) but followed the firing of somatosensory cortical neurons by about 9 ms (Fig. 6*D*).

The directionality of information flow between VPM-POm thalamic nuclei and the related cortical region was further analyzed by measuring the strength of association (h^2) and temporal delays between somatosensory cortex ECoG and thalamic intracellular signals (see Supplementary Methods). The degree of association between ECoG and thalamic intracellular activities was low (from 0.066 to 0.143; mean = 0.098 ± 0.005, n = 13 paired recordings) during interictal periods (Supplementary Fig. S1*A* and S1*B*). In both VPM and POm neurons, h^2 gradually increased just prior to the cortical SWD and was maintained at an elevated value (from 0.207 to 0.535; mean = 0.420 ± 0.026, n = 13 paired recordings; P < 0.001; paired t-test) during the seizure (Supplementary Fig. S1*A* and *B*). Higher values of h^2 during the seizure were

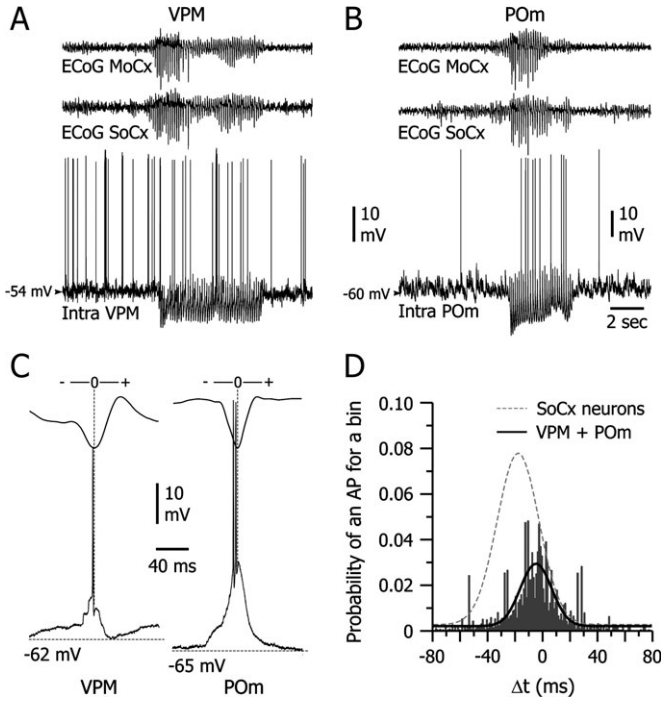

Figure 6. Intracellular activity of VPM and POm thalamic neurons during SWDs. (*A*) and (*B*) Intracellular activity of a VPM (*A*) and a POm (*B*) thalamic neuron (bottom traces) simultaneously recorded with the motor (MoCx) and the somatosensory (SoCx) ECoGs (top traces). Cortical SWDs were concomitant with large-amplitude membrane potential oscillations superimposed on a sustained hyperpolarization. (*C* and *D*) Temporal relationship between the firing of VPM and POm neurons and the corresponding ictal activity in the cerebral cortex. (*C*) Typical examples of simultaneous recordings from the intracellular activity (bottom) in VPM (left) and POm (right) neurons and from the spike-and-wave complexes in the corresponding somatosensory ECoG (top). (*D*) Histogram (gray bars) and Gauss–Laplace distribution (black line) of the timing (Δt) of all action potentials (AP; bin size = 1 ms) recorded in VPM and POm thalamic neurons ($n = 1155$ action potentials from 11 cells) relative to the SoCx ECoG spike component taken as the zero-time reference (as shown in *C*). The mean latency of the first action potential was -9.0 ± 0.7 ms ($n = 11$ cells). The dashed gray line represents the firing probability of somatosensory cortical neurons (data taken from Fig. 1*D*).

associated with more stable time delays. In 13 paired recordings (VPM-ECoG, $n = 5$; POm-ECoG, $n = 8$), oscillatory activity in VPM and POm thalamic cells lagged spike-and-wave activity in the somatosensory cortex by 7.7 ± 2.8 s during the first second of the seizure (Supplementary Fig. S1*A* and *C*). No preferential directional coupling was evident during the later components of the SWD (Supplementary Fig. S1*A* and *C*).

SWDs in the Somatosensory Cortex do not Require Paroxysmal Thalamic Oscillations

Arguing against the hypothesis that intrathalamic networks could be an important epileptogenic source (see Bessaih et al. 2006; Toth et al. 2007), we could record, in between seizures, short epochs (1.37 ± 0.15 s, $n = 16$) of paroxysmal oscillations (11.3 ± 0.6 Hz, $n = 16$) in the somatosensory and motor ECoGs (Fig. 7*A*), correlated with suprathreshold rhythmic depolarizations in the related cortical neurons (data not shown), which were not concomitant with robust membrane potential oscillations in the recorded thalamocortical neurons (3 POm cells and 1 VPM cells) (Fig. 7*B*). This lack of correlation between ECoGs and intracellular activities could be found in thalamic neurons that yet exhibited rhythmic membrane depolarizations in association with the full expression of cortical SWDs (Fig. 7*A*). These cells did not exhibit impairment in their intrinsic excitability, with typical current-induced firing patterns and membrane input resistance (40.0 ± 5.2 MΩ, $n = 4$ neurons) (Fig. 7*C*) similar ($P > 0.05$; unpaired *t*-test) to that of the overall neuronal population.

To ascertain whether the somatosensory cortex is capable of generating epileptic patterns in absence of thalamocortical inputs, we made unilateral intrathalamic injections of TTX at the boundary between POm and VPM nuclei ($n = 3$ experiments) and we simultaneously recorded local thalamic field potentials and ipsilateral somatosensory ECoGs (Fig. 8*A*). TTX injections abolished paroxysmal oscillations in the thalamus, whereas long sequences of spike-and-wave activity persisted in the somatosensory cortex, but with lower internal frequencies (6.9 ± 0.1 Hz, $n = 3$ GAERS) compared with control recordings (8.7 ± 0.3 Hz, $n = 3$; $P < 0.001$ in each experiment; Mann–Whitney rank sum test) (Fig. 8*B*). The specificity of TTX injection in the blockade of thalamic paroxysms was attested by the lack of thalamic field potential changes after intrathalamic vehicle injections (0.9% NaCl; 30 μL; $n = 2$ experiments) (Fig. 8*C*). Duration of cortical SWDs (before vehicle, 4.8 ± 0.8 s; after vehicle, 4.8 ± 0.9 s; $n = 2$ GAERS) as well as their internal frequency (before vehicle, 8.7 ± 1.2 Hz; after vehicle, 8.8 ± 0.9 Hz, $n = 2$) was not significantly modified by the vehicle injection ($P > 0.1$ for both parameters in each experiment; Mann–Whitney rank sum test).

Altogether, these findings demonstrate that somatosensory cortical SWDs can occur without concomitant paroxysms in the related thalamic nuclei, strongly refuting the hypothesis that thalamocortical projections could act as a causal factor for cortical seizures.

Lack of Paroxysmal Oscillations in Thalamocortical Cells following Inactivation of the Somatosensory Cortex

In 4 experiments, we investigated the effect of TTX application to somatosensory cortex on the intracellular activity of related thalamic neurons. In all cells tested (1 VPM and 3 POm cells), pharmacological blockade of somatosensory cortical SWDs resulted in the complete disappearance of paroxysmal membrane oscillations in thalamocortical neurons (Fig. 9*A*). This was concomitant with a decrease in the amplitude of membrane potential fluctuations (Fig. 9*A*), as attested by the reduced variability of membrane potential distributions after TTX application, in the absence of change in mean membrane potential (Control, –57.9 ± 1.0 mV, $n = 11$ cells; after TTX, –57.3 ± 1.3 mV, $n = 4$ cells; $P > 0.05$; unpaired *t*-test) (Fig. 9*B*). The extinction of thalamic ictal oscillations did not result from altered intrinsic properties of thalamic neurons, as their apparent input resistance (Control, 37.8 ± 2.8 MΩ, $n = 11$ cells; after TTX, 31.5 ± 7.2 MΩ, $n = 4$ cells; $P > 0.05$; unpaired *t*-test) and membrane time constant (Control, 13.9 ± 2.0 ms, $n = 11$ cells; after TTX, 9.7 ± 0.9 ms, $n = 4$ cells; $P > 0.05$; Mann–Whitney rank sum test) were not significantly modified after drug application. Moreover, action potentials, with amplitude, duration and voltage threshold similar to those measured in control conditions ($P > 0.05$ for all parameters) could be triggered in thalamic cells under cortical TTX treatment (Fig. 9*Ab*). This demonstrates that the drug did not spread to the recorded thalamic site and suggests that changes in

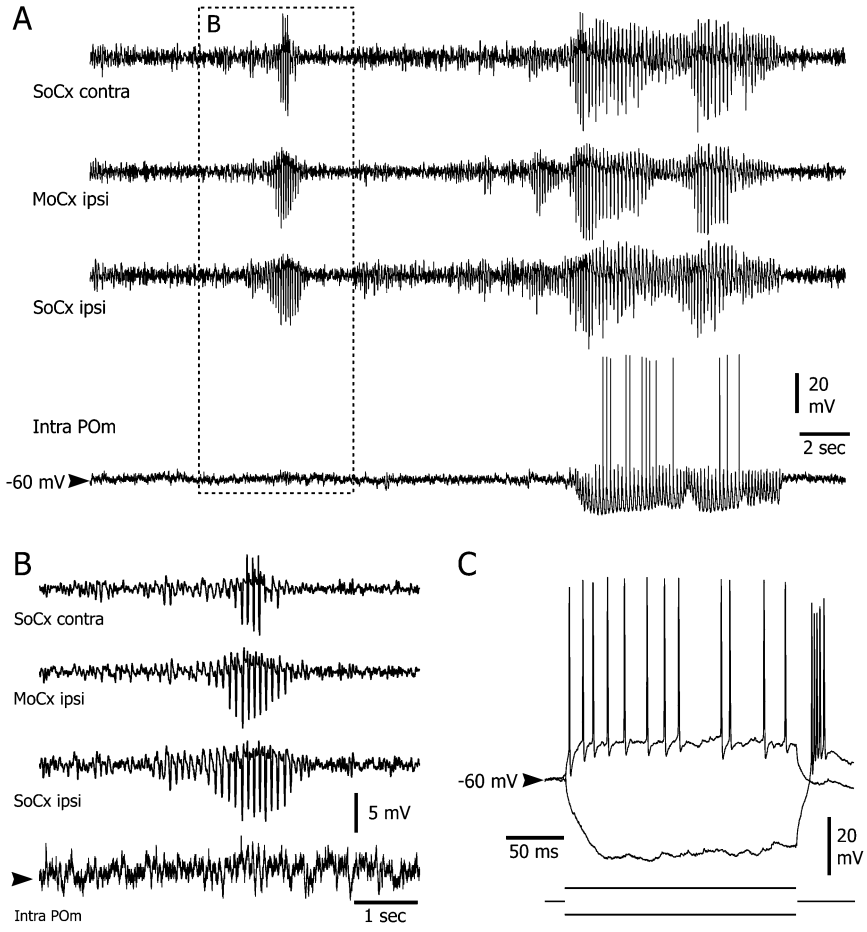

Figure 7. Lack of rhythmic activity in thalamocortical neurons during interictal ECoG paroxysmal oscillations. (*A* and B) Simultaneous recordings of ipsilateral motor (MoCx ipsi) and somatosensory (SoCx ipsi) ECoGs, contralateral somatosensory (SoCx contra) ECoG and of the intracellular activity of a POm thalamic neuron (Intra POm). The full expression of the SWD was correlated with robust oscillations in the intracellularly recorded thalamic neuron. However, as shown in (*B*) by the expansion of the record framed in (*A*), the occurrence in between seizures of paroxysmal ECoG oscillations (~10 Hz, 2.5 s of duration) had no reflection in the thalamic intracellular activity. (*C*) Voltage responses (top traces) to a hyperpolarizing (−0.8 nA) and depolarizing (+0.8 nA) current pulse (bottom traces) of the thalamic neuron illustrated in (*A*, *B*), showing the typical electrophysiological properties of thalamocortical neurons (see Fig. 5).

thalamic cell activity resulted exclusively from the loss of activity in cortical afferents.

Discussion

This study tested the hypothesis that the facial somatosensory cortex acts as a focal site for the initiation of generalized SWDs in the GAERS genetic model of absence seizures (Meeren et al. 2002; Depaulis and Van Luijtelaar 2005; Meeren et al. 2005; van Luijtelaar and Sitnikova 2006; Polack et al. 2007). Using intracellular and ECoG recordings in vivo, we obtained new evidence on several points. First, blockade of firing and synaptic activities in facial somatosensory cortical neurons, following topical application of TTX, suppresses paroxysmal discharges in 1) neurons and ECoG of the somatosensory cortex, 2) motor cortex ECoG, and 3) thalamocortical neurons in register with the somatosensory cortex. Second, an identical pharmacological inhibition within the motor cortex or the related thalamic nuclei did not abolish spike-and-wave activity in the somatosensory cortex. Third, somatosensory cortex could generate paroxysmal oscillations despite a lack of rhythmic discharge in the related thalamocortical cells. Finally, measurements of temporal relationships between ECoGs and intracellular signals indicate a consistent sequential activation of first the somatosensory cortex, then its thalamic targets and finally distant cortical areas during a seizure.

The Facial Somatosensory Cortex as a Cortical Focus for Absence Seizures: Experimental Evidence

An epileptic focus is defined by a number of anatomo-functional properties which promote the initiation of ictal activity which then propagates to distant brain regions. These local ictogenic properties can be summarized as follows: 1) the existence in a restricted cerebral region of network and/or cellular alterations contributing to excessive, hypersynchronous activity, 2) paroxysmal firing of ictogenic cells can initiate epileptic discharges at remote sites to ensure seizure propagation, and 3) the functional inactivation of the focal region, or its anatomical resection, suppresses local and propagated seizure activity. According to these criteria, the present findings strongly support the hypothesis that the facial somatosensory cortex of GAERS contains an epileptic focus where SWDs are initiated and then spread throughout cortico-thalamic networks. Our intracellular recordings demonstrate that during and in between spike-and-wave activity deep-layer

neurons of the facial somatosensory cortex discharge at frequencies significantly higher than do neurons of the motor cortex. Moreover, ictal discharges in somatosensory cortical cells precede by about 12 ms the corresponding firing in motor cortex neurons (see Fig. 1*D*). These results confirm previous findings obtained in GAERS showing that layer 5/6 neurons of the facial somatosensory cortex exhibit a distinctive hyperactivity and lead the firing of remote cortical cells during the epileptic discharge (Polack et al. 2007). The directional propagation of cortical seizure activity from the somatosensory area to distant cerebral regions is further supported by our pharmacological experiments. SWDs in the motor cortex disappeared following TTX application to the somatosensory region, but an identical treatment of motor cortex had no effect on epileptic activity in somatosensory cortex. Consistently, it has been shown in WAG/Rij rats and GAERS that epileptic discharges are suppressed by microinjection of sodium channel blockers, such as lidocaine (Sitnikova and van Luijtelaar 2004) or phenytoin (Gurbanova et al. 2006), in the primary somatosensory cortex. However, in these studies, the effect of the drugs on the activity of cortical focus neurons was not demonstrated and the impact of the inactivation of remote cortical regions was not investigated. The ability of ethosuximide, a anti-absence drug, to abolish SWDs when applied into the peri-oral region of the primary sensory cortex of GAERS also support the involvement of this brain region in the initiation of absence seizures (Manning et al. 2004).

The persistence of residual "ictal-like" oscillations in the untreated hemisphere after complete abolition of SWDs by TTX application to the other, may point to an involvement of crossed interactions between somatosensory cortical areas in the genesis of spike-and-wave activity (see Fig. 3*Ab*). This finding, together with the disruption of coherent SWDs between both hemispheres after callosotomy in GAERS (Vergnes et al. 1989), indicate that both somatosensory cortices have ictogenic properties but that the full expression and bilateral synchronization of spike-and-wave activities require functional interactions between both foci.

The leading role of cortical somatosensory neurons in the related corticothalamic loop during SWDs is further demonstrated by our intracellular recordings of VPM and POm thalamocortical cells showing a delayed firing (~ +9 ms, see Fig. 6*D*) relative to somatosensory cortex neurons. Moreover, interictal and ictal firing rates of thalamic cells were considerably lower than those of corresponding corticothalamic neurons. In addition, multisite local field potentials from the

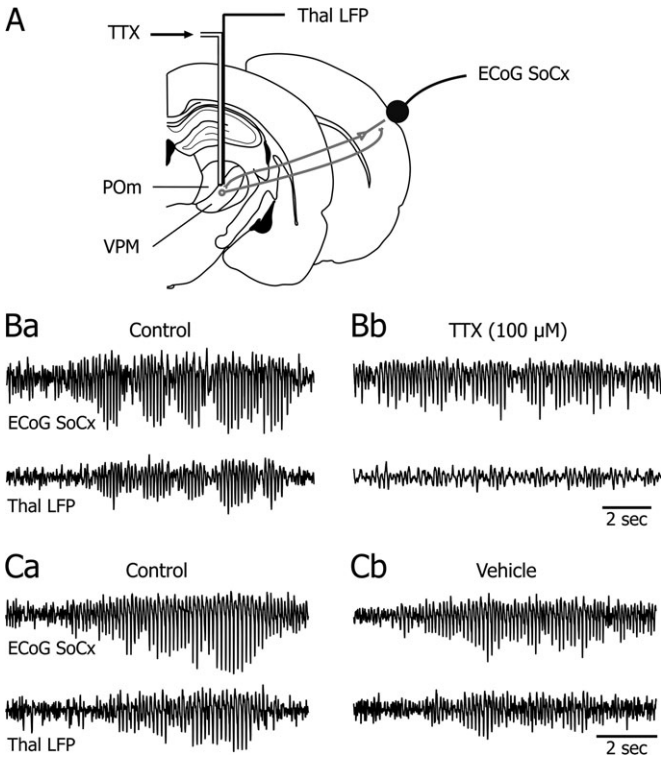

Figure 8. Persistence of SDWs in the somatosensory cortex after intrathalamic injection of TTX. (*A*) Experimental arrangement. Injection of TTX (30 µL, 100µM) was made at the boundary of POm and VPM thalamic nuclei. Thalamic (Thal) local field potential (LFP) was recorded at the vicinity of the injection site and ECoG of the ipsilateral somatosensory cortex (SoCx) was simultaneously recorded. (*B*) Cortical SWDs persisted after intrathalamic injection of TTX. (*Ba*) Paired recordings of somatosensory ECoG (top trace) and thalamic field potential (bottom trace) before TTX injection. Note that cortical SWDs were correlated with paroxysmal thalamic oscillations. (*Bb*) TTX injection resulted after 10 min in a disappearance of thalamic oscillations (bottom trace) whereas the corresponding ECoG still exhibited sustained spike-and-wave activity (top trace). Calibration in (*Bb*) applies to (*Ba*). (*C*) Intrathalamic application of a vehicle solution did not affect neither the thalamic oscillations nor cortical SWDs. Examples of cortical (top traces) and thalamic (bottom traces) recordings in control (*Ca*) and 10 min after vehicle injection. Calibration in (*Cb*) applies to (*Ca*). Results depicted in (*B*) and (*C*) are from 2 separated experiments.

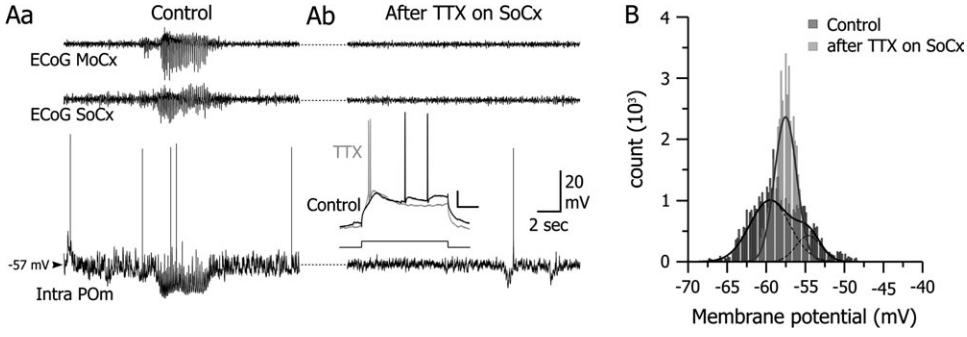

Figure 9. TTX application on the somatosensory cortex suppresses paroxysmal oscillations in thalamocortical neurons. (*A*) Simultaneous recordings of motor and somatosensory ECoGs and of the intracellular activity of a POm thalamic neuron, before (*Aa*) and after (*Ab*) local application of TTX on the somatosensory cortex. Inset, superimposition of suprathreshold voltage responses (top traces) of a thalamic neuron to depolarizing current pulses (bottom trace) in control (black trace) and after TTX application on SoCx (gray trace). Calibration bars: 10 mV, 50 ms. (*B*) distributions of membrane potential values (bin = 0.2 mV; continuous record of 5 s) during interictal periods, in control (dark gray) and after pharmacological interruption of SWDs (light gray). Control histogram was best fitted by a bimodal Gauss–Laplace fit (black line, centers: −59.5 ± 5.1 mV and −54.6 ± 3.3 mV, r^2 = 0.703), whereas TTX treatment led to a narrow unimodal Gauss–Laplace curve (gray line, center = −57.5 ± 2.7 mV, r^2 = 0.775).

freely moving GAERS showed that the occurrence of SWDs in the ventrobasal complex of the thalamus systematically follows the appearance of paroxysmal activities in the somatosensory cortex (Polack et al. 2007). Consistently, we showed in the present study the complete disappearance of paroxysmal oscillations in VPM and POm thalamic neurons following pharmacological inactivation of the somatosensory cortex. A further demonstration of the ability of cerebral cortex to generate epileptic-like activity in absence of thalamic oscillations was the occurrence of spontaneous ECoG paroxysms without counterpart in thalamic neurons (see Fig. 7*A*,*B*). This is also confirmed by the persistence of cortical spike-and-wave activity after functional inactivation of the related thalamic nuclei (see Fig. 8), a finding consistent with the long sequences of continuous cortical spike-and-wave activity in the athalamic cat with cortical seizures (Steriade and Contreras 1998).

Altogether, these findings agree with previous studies suggesting a prominent role of cortical neurons in thalamocortical epileptic oscillations in GAERS (Pinault 2003) and in the cat pharmacological model of spike-and-wave activity (Steriade and Contreras 1998) and refute the possibility that absence seizures are initiated in the thalamus (see Bessaih et al. 2006; Toth et al. 2007). However, although corticothalamic SWDs in GAERS arise from the deep-layer neurons of the cortical focus (Polack et al. 2007; present study), we cannot exclude that the epileptic discharges in these ictogenic neurons are, at least partially, under control of neuronal inputs external to the corticothalamic loop.

Putative Mechanisms of Initiation, Generalization, and Termination of SWDs

Although several lines of evidence indicate that SWDs are initiated from the somatosensory region of cortex in rodent genetic models of absence epilepsy (Meeren et al. 2002, 2005; Manning et al. 2004; van Luijtelaar and Sitnikova 2006; Polack et al. 2007; present study), the cellular and network ictogenic mechanisms remain unclear.

In WAG/Rij rats, an abnormal pattern of dendritic arborizations has been demonstrated in primary somatosensory cortex (Karpova et al. 2005). However, no anomalous morphological properties were apparent for the different neuronal populations in the homologous epileptic zone of GAERS (Polack et al. 2007).

Alternatively, the abnormal hyperactivity of somatosensory cortical layer 5/6 neurons (Polack et al. 2007, see also Fig. 1*A* vs. *B*), as well as their propensity to generate epileptic oscillations, could result from a dysregulation in their intrinsic and/or synaptic properties. A consistent feature of cortical neurons activity during SWDs, including that of deep-layer neurons of the focus, is the maintenance of a sustained membrane hyperpolarization (Charpier et al. 1999; Paz et al. 2005, 2007; Polack and Charpier 2006; Polack et al. 2007; present study). This is likely due to a transient interruption of the tonic excitatory synaptic drive, leading to a cell polarization toward the resting potential and an increase in membrane input resistance (Charpier et al. 1999), both favoring rhythmic synaptic depolarizations and postinhibitory rebounds of intrinsic excitation. The exacerbated activity of deep-layer neurons of the cortical focus could be due to an increased expression of voltage-gated sodium channels (Klein et al. 2004), which may cause elevated tonic and bursting activities and favor the occurrence of SWDs (Blumenfeld and McCormick 2000). A reduction in the dendritic I_h current, as found in pyramidal neurons of WAG/Rij rats (Strauss et al. 2004; Kole et al. 2007), would facilitate the temporal summation of repetitive synaptic inputs (Strauss et al. 2004) and the generation of high-frequency burst firing (Kole et al. 2007). Such modifications in membrane excitability could act in synergy with changes in synaptic systems to promote epileptic discharges. For instance, a decrease in $GABA_A$ receptor-mediated synaptic transmission, associated with an increase in glutamatergic NMDA-dependent conductances, as found in the deep layers of WAG/Rij rats' focus (D'Antuono et al. 2006), provides a powerful potential mechanism for inducing and/or amplifying paroxysmal activities within the somatosensory cortex.

Once the SWD is initiated in the cortical focus, epileptic discharges rapidly propagate to the intracortical networks and related thalamic regions, dynamic processes that will engage the corticothalamocortical loops in abnormal synchronized oscillations. It is likely that the relative low firing rate in most thalamocortical cells during spike-and-wave activity (Pinault et al. 1998; Charpier et al. 1999; Pinault 2003; Timofeev and Steriade 2004; Polack and Charpier 2006; Paz et al. 2007; see also Figures 6*A*,*B* and 7*A*) originate from a powerful GABAergic inhibition arising from the bursting of nucleus reticularis thalami neurons (Slaght et al. 2002; Pinault 2003; Timofeev and Steriade 2004), which are mainly driven by their cortical inputs. However, in the few active thalamocortical neurons, the SWD-associated hyperpolarization deinactivates I_T and the resulting low-threshold calcium potential, in association with cortical synaptic inputs, will be able to generate repetitive bursting (Pinault 2003; Polack and Charpier 2006; Paz et al. 2007; see also Fig. 6*A*–*C*). Transmission of this rhythmic thalamic excitation to the cerebral cortex may tend to reinforce coherent seizure activity in widespread cortical areas, including the focal region. This hypothesis is consistent with the slight slowing of cortical focus spike-and-wave activity after pharmacological blockade of thalamocortical inputs (see Fig. 8).

Mechanisms for the termination of spike-and-wave activity remain enigmatic (Timofeev and Steriade 2004). It is plausible that paroxysmal discharges during SWDs (see Fig. 1*A*) induce an intracellular calcium influx, that would tend to activate calcium-dependent potassium currents (Sah and Faber 2002), decreasing cellular excitability and interrupting epileptic activities (Timofeev and Steriade 2004). A decreased extracellular calcium concentration would also tend to weaken synaptic transmission (Katz and Miledi 1970), and might also contribute to SWD termination (Massimini and Amzica 2001). Alternatively, the transition from ictal to resting state could be controlled by a negative feedback due to a slow adaptation sodium-dependent potassium current (Compte et al. 2003). In addition to these ionic changes, recent in vivo investigations in GAERS strongly suggest that the basal ganglia, via their feedback pathway to the cerebral cortex, provide an on-line control system for absence seizures (Deransart and Depaulis 2002; Slaght et al. 2004; Paz et al. 2005, 2007). Specifically, the propagation of cortical epileptic discharges through the basal ganglia circuits (Slaght et al. 2004; Paz et al. 2005, 2007) should act to desynchronize activity in their thalamocortical neuronal targets, decreasing cellular excitability in the cerebral cortex and thus contributing to seizure termination (Paz et al. 2007). Such a participation of thalamocortical inputs in the expression of cortical SWDs is also supported by our results showing that the inactivation of thalamic nuclei, related to the cortical focus,

results into long sequences of spike-and-wave activity in the facial somatosensory ECoG (see Fig. 8*Bb*).

Toward a Novel Electroclinical Classification of Absence Epilepsy?

An increasing number of experimental investigations in pharmacological and genetic models of absence epilepsy, including the present study, indicate that the cerebral cortex plays a fundamental role in the initiation of SWDs with a focal onset from a restricted cortical region. In human patients, the "generalized" nature of absence seizures may be a clinical convention rather than a concept firmly based on electroencephalographic evidence. For instance, an accurate source analysis from dense-array surface electrodes demonstrates that the onset of absence seizures in human is associated with early activation of discrete, often unilateral, frontal or orbital cortical areas (Holmes et al. 2004). The authors concluded that absence seizures in these patients were not truly "generalized," with immediate and global cortical involvement, but rather were initiated, then propagated, from specific cortical networks (Holmes et al. 2004). This hypothesis is supported by recent data showing that surface electrical paroxysms in human absence seizures did not have a "generalized onset" but rather were initiated by focal discharges largely restricted to the frontal cortex (Sadleir et al. 2006).

The reconciliation of experimental and clinical findings, that absence seizures are not "generalized" in the sense of homogenous and simultaneous cortical activation but involve local ictogenic processes within a confined cortical region, might eventually lead to a reconsideration of the electroclinical classification of absence epilepsy.

Supplementary Material

Supplementary material can be found at: http://www.cercor.oxfordjournals.org/.

Funding

Agence Nationale de la Recherche grants (ANR RO6275CS, 2006); the Institut National de la Santé et de la Recherche Médicale; the Fondation Française pour la Recherche sur l'Epilepsie; and the Ligue Française Contre l'Epilepsie and Pfizer doctoral fellowship supported P.-O.P.

Notes

We thank Anne-Marie Godeheu for histological processing, Richard Miles, Antoine Depaulis and Morgane Pidoux for critical reading of the manuscript, and Jean-Michel Deniau and Nicolas Maurice for constructive discussions and HRP expertise. We also thank the expert referees for their thoughtful and helpful comments. *Conflict of Interest*: None declared.

Address correspondence to Stephane Charpier, PhD, Institut National de la Santé et de la Recherche Médicale – Unité 667, Collège de France, 11, place Marcelin Berthelot, 75231 Paris, Cedex 05, France. Email: stephane.charpier@college-de-france.fr.

References

Avanzini G, Panzica F, de Curtis M. 2000. The role of the thalamus in vigilance and epileptogenic mechanisms. Clin Neurophysiol. 111(Suppl. 2):S19–S26.

Bal T, von Krosigk M, McCormick DA. 1995. Role of the ferret perigeniculate nucleus in the generation of synchronized oscillations in vitro. J Physiol. 483(Pt 3):665–685.

Bessaih T, Bourgeais L, Badiu CI, Carter DA, Toth TI, Ruano D, Lambolez B, Crunelli V, Leresche N. 2006. Nucleus-specific abnormalities of GABAergic synaptic transmission in a genetic model of absence seizures. J Neurophysiol. 96:3074–3081.

Blumenfeld H, McCormick DA. 2000. Corticothalamic inputs control the pattern of activity generated in thalamocortical networks. J Neurosci. 20:5153–5162.

Bruno RM, Khatri V, Land PW, Simons DJ. 2003. Thalamocortical angular tuning domains within individual barrels of rat somatosensory cortex. J Neurosci. 23:9565–9574.

Buzsaki G. 1991. The thalamic clock: emergent network properties. Neuroscience. 41:351–364.

Charpier S, Leresche N, Deniau JM, Mahon S, Hughes SW, Crunelli V. 1999. On the putative contribution of GABA(B) receptors to the electrical events occurring during spontaneous spike and wave discharges. Neuropharmacology. 38:1699–1706.

Coenen AM, van Luijtelaar EL. 2003. Genetic animal models for absence epilepsy: a review of the WAG/Rij strain of rats. Behav Genet. 33:635–655.

Compte A, Sanchez-Vives MV, McCormick DA, Wang XJ. 2003. Cellular and network mechanisms of slow oscillatory activity (<1 Hz) and wave propagations in a cortical network model. J Neurophysiol. 89:2707–2725.

D'Antuono M, Inaba Y, Biagini G, D'Arcangelo G, Tancredi V, Avoli M. 2006. Synaptic hyperexcitability of deep layer neocortical cells in a genetic model of absence seizures. Genes Brain Behav. 5:73–84.

D'Arcangelo G, D'Antuono M, Biagini G, Warren R, Tancredi V, Avoli M. 2002. Thalamocortical oscillations in a genetic model of absence seizures. Eur J Neurosci. 16:2383–2393.

D'Arcangelo G, D'Antuono M, Tancredi V, Avoli M. 2006. Neocortical hyperexcitability in a genetic model of absence seizures and its reduction by levetiracetam. Epilepsia. 47:1144–1152.

Danober L, Deransart C, Depaulis A, Vergnes M, Marescaux C. 1998. Pathophysiological mechanisms of genetic absence epilepsy in the rat. Prog Neurobiol. 55:27–57.

Depaulis A, Van Luijtelaar EL. 2005. Genetic models of absence epilepsy in the rat. In: Pitkänen A, Schwartzkroin PA, Moshé SL, editors. Models of seizures and epilepsy. London: Elsevier Academic Press. p. 233–248.

Deransart C, Depaulis A. 2002. The control of seizures by the basal ganglia? A review of experimental data. Epileptic Disord. 4(Suppl. 3):S61–S72.

Deransart C, Hellwig B, Heupel-Reuter M, Leger JF, Heck D, Lucking CH. 2003. Single-unit analysis of substantia nigra pars reticulata neurons in freely behaving rats with genetic absence epilepsy. Epilepsia. 44:1513–1520.

Destexhe A, Pare D. 1999. Impact of network activity on the integrative properties of neocortical pyramidal neurons in vivo. J Neurophysiol. 81:1531–1547.

Destexhe A, Sejnowski TJ. 2003. Interactions between membrane conductances underlying thalamocortical slow-wave oscillations. Physiol Rev. 83:1401–1453.

Emmers R. 1988. Somesthetic system of the rat. New York: Raven Press.

Fricker D, Verheugen JA, Miles R. 1999. Cell-attached measurements of the firing threshold of rat hippocampal neurones. J Physiol. 517(Pt 3): 791–804.

Gurbanova AA, Aker R, Berkman K, Onat FY, van Rijn CM, van Luijtelaar G. 2006. Effect of systemic and intracortical administration of phenytoin in two genetic models of absence epilepsy. Br J Pharmacol. 148:1076–1082.

Holmes MD, Brown M, Tucker DM. 2004. Are "generalized" seizures truly generalized? Evidence of localized mesial frontal and frontopolar discharges in absence. Epilepsia. 45:1568–1579.

Jahnsen H, Llinás R. 1984a. Electrophysiological properties of guinea-pig thalamic neurones: an in vitro study. J Physiol. 349:205–226.

Jahnsen H, Llinás R. 1984b. Ionic basis for electroresponsiveness and oscillatory properties of guinea-pig thalamic neurones in vitro. J Physiol. 349:227–247.

Karpova AV, Bikbaev AF, Coenen AM, van Luijtelaar G. 2005. Morphometric Golgi study of cortical locations in WAG/Rij rats: the cortical focus theory. Neurosci Res. 51:119–128.

Katz B, Miledi R. 1970. Further study of the role of calcium in synaptic transmission. J Physiol. 207:789–801.

Klein JP, Khera DS, Nersesyan H, Kimchi EY, Waxman SG, Blumenfeld H. 2004. Dysregulation of sodium channel expression in cortical neurons in a rodent model of absence epilepsy. Brain Res. 1000:102–109.
Kole MH, Brauer AU, Stuart GJ. 2007. Inherited cortical HCN1 channel loss amplifies dendritic calcium electrogenesis and burst firing in a rat absence epilepsy model. J Physiol. 578:507–525.
Mahon S, Deniau JM, Charpier S. 2003. Various synaptic activities and firing patterns in cortico-striatal and striatal neurons in vivo. J Physiol Paris. 97:557–566.
Manning JP, Richards DA, Leresche N, Crunelli V, Bowery NG. 2004. Cortical-area specific block of genetically determined absence seizures by ethosuximide. Neuroscience. 123:5–9.
Marescaux C, Vergnes M, Depaulis A. 1992. Neurotransmission in rats' spontaneous generalized nonconvulsive epilepsy. Epilepsy Res Suppl. 8:335–343.
Massimini M, Amzica F. 2001. Extracellular calcium fluctuations and intracellular potentials in the cortex during the slow sleep oscillation. J Neurophysiol. 85:1346–1350.
McCormick DA, Pape HC. 1990. Properties of a hyperpolarization-activated cation current and its role in rhythmic oscillation in thalamic relay neurones. J Physiol. 431:291–318.
Meeren H, van Luijtelaar G, Lopes da Silva F, Coenen A. 2005. Evolving concepts on the pathophysiology of absence seizures: the cortical focus theory. Arch Neurol. 62:371–376.
Meeren HK, Pijn JP, van Luijtelaar EL, Coenen AM, Lopes da Silva FH. 2002. Cortical focus drives widespread corticothalamic networks during spontaneous absence seizures in rats. J Neurosci. 22:1480–1495.
Mesulam MM. 1978. Tetramethyl benzidine for horseradish peroxidase neurohistochemistry: a non-carcinogenic blue reaction product with superior sensitivity for visualizing neural afferents and efferents. J Histochem Cytochem. 26:106–117.
Myers RD. 1966. Injection of solutions into the cerebral tissue: relation between volume and diffusion. Physiol Behav. 1:171–174.
Panayiotopoulos CP. 1997. Absence epilepsies. In: Engel J, Pedley TA, editors. Epilepsy: a comprehensive textbook. Philadelphia: Lippincot-Raven. p. 2327–2346.
Papadopoulos MC, Kim JK, Verkman AS. 2005. Extracellular space diffusion in central nervous system: anisotropic diffusion measured by elliptical surface photobleaching. Biophys J. 89:3660–3668.
Pare D, Shink E, Gaudreau H, Destexhe A, Lang EJ. 1998. Impact of spontaneous synaptic activity on the resting properties of cat neocortical pyramidal neurons in vivo. J Neurophysiol. 79: 1450–1460.
Paxinos G, Watson C. 1986. The brain in stereotaxic coordinates. Sydney: Academic Press.
Paz JT, Chavez M, Saillet S, Deniau JM, Charpier S. 2007. Activity of ventral medial thalamic neurons during absence seizures and modulation of cortical paroxysms by the nigrothalamic pathway. J Neurosci. 27:929–941.
Paz JT, Deniau JM, Charpier S. 2005. Rhythmic bursting in the cortico-subthalamo-pallidal network during spontaneous genetically determined spike and wave discharges. J Neurosci. 25:2092–2101.
Pinault D. 2003. Cellular interactions in the rat somatosensory thalamocortical system during normal and epileptic 5-9 Hz oscillations. J Physiol. 552:881–905.
Pinault D, Leresche N, Charpier S, Deniau JM, Marescaux C, Vergnes M, Crunelli V. 1998. Intracellular recordings in thalamic neurones during spontaneous spike and wave discharges in rats with absence epilepsy. J Physiol. 509(Pt 2):449–456.
Polack PO, Charpier S. 2006. Intracellular activity of cortical and thalamic neurones during high-voltage rhythmic spike discharge in Long-Evans rats in vivo. J Physiol. 571:461–476.
Polack PO, Guillemain I, Hu E, Deransart C, Depaulis A, Charpier S. 2007. Deep layer somatosensory cortical neurons initiate spike-and-wave discharges in a genetic model of absence seizures. J Neurosci. 27:6590–6599.
Rall W. 1969. Time constants and electrotonic length of membrane cylinders and neurons. Biophys J. 9:1483–1508.
Sadleir LG, Farrell K, Smith S, Connolly MB, Scheffer IE. 2006. Electroclinical features of absence seizures in childhood absence epilepsy. Neurology. 67:413–418.
Sah P, Faber ES. 2002. Channels underlying neuronal calcium-activated potassium currents. Prog Neurobiol. 66:345–353.
Sawyer SF, Young SJ, Groves PM. 1989. Quantitative Golgi study of anatomically identified subdivisions of motor thalamus in the rat. J Comp Neurol. 286:1–27.
Seidenbecher T, Staak R, Pape HC. 1998. Relations between cortical and thalamic cellular activities during absence seizures in rats. Eur J Neurosci. 10:1103–1112.
Sherman SM. 2001. Tonic and burst firing: dual modes of thalamocortical relay. Trends Neurosci. 24:122–126.
Simons DJ, Carvell GE. 1989. Thalamocortical response transformation in the rat vibrissa/barrel system. J Neurophysiol. 61:311–330.
Sitnikova E, van Luijtelaar G. 2004. Cortical control of generalized absence seizures: effect of lidocaine applied to the somatosensory cortex in WAG/Rij rats. Brain Res. 1012:127–137.
Slaght SJ, Leresche N, Deniau JM, Crunelli V, Charpier S. 2002. Activity of thalamic reticular neurons during spontaneous genetically determined spike and wave discharges. J Neurosci. 22:2323–2334.
Slaght SJ, Paz T, Chavez M, Deniau JM, Mahon S, Charpier S. 2004. On the activity of the corticostriatal networks during spike-and-wave discharges in a genetic model of absence epilepsy. J Neurosci. 24:6816–6825.
Steriade M, Contreras D. 1995. Relations between cortical and thalamic cellular events during transition from sleep patterns to paroxysmal activity. J Neurosci. 15:623–642.
Steriade M, Contreras D. 1998. Spike-wave complexes and fast components of cortically generated seizures. I. Role of neocortex and thalamus. J Neurophysiol. 80:1439–1455.
Steriade M, Jones EG, McCormick DA. 1997. Thalamus: organisation and function. Oxford: Elsevier Science.
Strauss U, Kole MH, Brauer AU, Pahnke J, Bajorat R, Rolfs A, Nitsch R, Deisz RA. 2004. An impaired neocortical Ih is associated with enhanced excitability and absence epilepsy. Eur J Neurosci. 19:3048–3058.
Timofeev I, Steriade M. 2004. Neocortical seizures: initiation, development and cessation. Neuroscience. 123:299–336.
Toth TI, Bessaih T, Leresche N, Crunelli V. 2007. The properties of reticular thalamic neuron GABA(A) IPSCs of absence epilepsy rats lead to enhanced network excitability. Eur J Neurosci. 26:1832–1844.
van Luijtelaar G, Sitnikova E. 2006. Global and focal aspects of absence epilepsy: the contribution of genetic models. Neurosci Biobehav Rev. 30:983–1003.
Vergnes M, Marescaux C, Lannes B, Depaulis A, Micheletti G, Warter JM. 1989. Interhemispheric desynchronization of spontaneous spike-wave discharges by corpus callosum transection in rats with petit mal-like epilepsy. Epilepsy Res. 4:8–13.